Modelling atmospheric flows with adaptive moving meshes

Christian Kühnlein[1], Piotr K. Smolarkiewicz [2], Andreas Dörnbrack [3]

[1]Ludwig-Maximilans-Universität München, Chair of Theoretical Meteorology, Munich, Germany

[2]National Center of Atmospheric Research, Boulder, CO, USA

[3]Deutsches Zentrum für Luft- und Raumfahrt, Insitut für Physik der Atmosphäre, Oberpfaffenhofen, Germany

June 26, 2012

Multiscale atmospheric flows

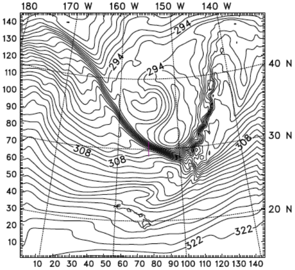

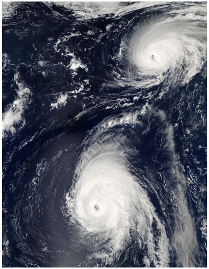

→ Processes of highly different local scales

→ Standard approach in atmospheric solvers of uniform mesh not optimal

→ Variable mesh applying locally finer/coarser resolution more efficient

→ Solution-adaptive mesh is able to conform to flow evolution

Combining the anelastic NFT solver with adaptive moving meshes

→ Build on previous works (Prusa and Smolarkiewicz, JCP 2003; ...), and extend EULAG's dynamical core with a solution-adaptive mesh capability (Kühnlein et al., JCP 2012):

- Implement moving mesh partial differential equations (MMPDEs) for solution-adaptive mesh generation (i.e. r-adaptivity)
- Effectively couple MMPDEs with non-oscillatory forward-in-time (NFT) solver underlying EULAG and its time-dependent generalised coordinate framework
- Verify adaptive solver for simple problem (scalar advection in 2D) and more complex atmospheric flow (baroclinic wave life cycles experiments in 3D). Testing of possible mesh refinement criteria

EULAG model formulation

→ Foundation of mesh adaptivity is time-dependent curvilinear coordinate framework:

$$(\bar{t}, \bar{\mathbf{x}}) \equiv (t, \mathcal{F}(t, \mathbf{x})) : \quad \mathcal{D}_p \rightarrow \mathcal{D}_t$$

- $\mathcal{D}_p$ is subdomain of physical space $\mathbf{S}_p$ with coordinates $(t, \mathbf{x}) \equiv (t, x, y, z)$
- $\mathcal{D}_t$ is subdomain of transformed computational space $\mathbf{S}_t$ with coordinates $(\bar{t}, \bar{\mathbf{x}}) \equiv (\bar{t}, \bar{x}, \bar{y}, \bar{z})$

- Specific mapping in current implementation of EULAG:

$$\mathcal{F}(t, \mathbf{x}) = (E(t, x, y), D(t, x, y), C(t, x, y, z))$$

→ Time-dependent vertical Gal-Chen coordinate (Prusa et al., JAS 1996; Wedi and Smolarkiewicz, JCP 2004)

→ Horizontal mapping considered for moving mesh adaptivity

EULAG model formulation

→ Foundation of mesh adaptivity is time-dependent curvilinear coordinate framework:

$$(\bar{t}, \bar{\mathbf{x}}) \equiv (t, \mathcal{F}(t, \mathbf{x})) : \quad \mathcal{D}_p \rightarrow \mathcal{D}_t$$

- $\mathcal{D}_p$ is subdomain of physical space $\mathbf{S}_p$ with coordinates $(t, \mathbf{x}) \equiv (t, x, y, z)$
- $\mathcal{D}_t$ is subdomain of transformed computational space $\mathbf{S}_t$ with coordinates $(\bar{t}, \bar{\mathbf{x}}) \equiv (\bar{t}, \bar{x}, \bar{y}, \bar{z})$

- Specific mapping in current implementation of EULAG:

$$\mathcal{F}(t, \mathbf{x}) = (E(t, x, y), D(t, x, y), C(t, x, y, z))$$

→ Time-dependent vertical Gal-Chen coordinate (Prusa et al., JAS 1996; Wedi and Smolarkiewicz, JCP 2004)

→ Horizontal mapping considered for moving mesh adaptivity

EULAG model formulation

→ Strong conservation form of anelastic equations (Lipps and Hemler, JAS 1982) in time-dependent generalised coordinates (Prusa and Smolarkiewicz, JCP 2003; Wedi and Smolarkiewicz, JCP 2004; Kühnlein etal., JCP 2012;...):

$$\frac{\partial(\rho^* v^j)}{\partial \overline{t}} + \frac{\partial(\rho^* \overline{v}^{*k} v^j)}{\partial \overline{x}^k} = -\rho^* \widetilde{G}_j^k \frac{\partial \pi'}{\partial \overline{x}^k} + \rho^* g \frac{\theta'}{\theta_b} \delta_3^j - \rho^* \varepsilon_{jik} f_i \, v'^k - \rho^* \, \alpha_M \, v'^j$$

$$\frac{\partial(\rho^* \theta')}{\partial \overline{t}} + \frac{\partial(\rho^* \overline{v}^{*k} \theta')}{\partial \overline{x}^k} = -\rho^* \overline{v}^{s^k} \frac{\partial \theta_e}{\partial \overline{x}^k} - \rho^* \, \alpha_H \, \theta'$$

$$\frac{\partial(\rho^* \overline{v}^{s^k})}{\partial \overline{x}^k} = 0$$

- Three different velocities: v^j (physical), $\overline{v}^{*k} = d\overline{x}^k / d\overline{t}$ (contravariant), $\overline{v}^{s^k} = \overline{v}^{*k} - \overline{v}^{g^k}$ (solenoidal)
- Generalised density $\rho^* \equiv \rho_b \overline{G}$ product of background density ρ_b and Jacobian $\overline{G}$
- $\widetilde{G}_j^k$ represents elements of Jacobian matrix

EULAG model formulation

- generic Eulerian conservation law for prognostic equations

$$\frac{\partial(\rho^* \psi)}{\partial \bar{t}} + \overline{\nabla} \cdot \left(\rho^* \, \overline{\mathbf{v}}^* \, \psi\right) = \rho^* R^{\psi} \qquad \text{where} \qquad \overline{\nabla} \equiv \partial/\partial \overline{\mathbf{x}} \; , \; \overline{\mathbf{v}}^* = d\overline{\mathbf{x}}/d\bar{t}$$

- numerical solution algorithm on regular computational grid $(\bar{t}^n, \overline{\mathbf{x}}_{\mathbf{i}})$:

$$\psi_{\mathbf{i}}^{n+1} = \mathcal{A}_{\mathbf{i}}(\widetilde{\psi}) + 0.5\, \delta\bar{t}\, R^{\psi}|_{\mathbf{i}}^{n+1} \qquad \text{with} \qquad \widetilde{\psi} \equiv \psi^n + 0.5\, \delta\bar{t}\, R^{\psi}|^{n}$$

→ solution algorithm fully implicit with respect to dependent variables

→ $\mathcal{A}$ symbolises non-oscillatory forward-in-time advection transport scheme

→ implicit system solved iteratively using preconditioned GCR(k) solver

(Smolarkiewicz and Margolin, JCP 1998; Prusa and Smolarkiewicz, JCP 2003; ...)

⇒ $\mathcal{A}$ is flux-form second-order-accurate multidimensional advection transport algorithm MPDATA in this work

⇒ MPDATA requires $\mathcal{O}(\delta t^2)$ estimate of contravariant momentum flux $(\rho^* \overline{\mathbf{v}}^*)^{n+1/2}$

Moving mesh apparatus

MMPDEs (see Huang, JCP 2001) govern time-dependent mapping of horizontal coordinates from transformed to physical space $\mathbf{x}_h = \mathbf{x}_h(\overline{\mathbf{x}}_h, \overline{t})$:

$$P(\mathbf{x}_h, M)\,\frac{\partial \mathbf{x}_h}{\partial \overline{t}} = \sum_{i,j=1,2} D_{ij}(\mathbf{x}_h, M)\,\frac{\partial^2 \mathbf{x}_h}{\partial \overline{x}^i \partial \overline{x}^j} + \sum_{i=1,2} C_i(\mathbf{x}_h, M)\,\frac{\partial \mathbf{x}_h}{\partial \overline{x}^i}$$

with coefficients

$$D_{ij}(\mathbf{x}_h, M) = \nabla_h\,\overline{x}^i \cdot M^{-1}\,\nabla_h\,\overline{x}^j\ , \qquad C_i(\mathbf{x}_h, M) = -\nabla_h\,\overline{x}^i \cdot \left(\sum_{k=1,2} \frac{\partial M^{-1}}{\partial \overline{x}^k}\,\nabla_h\,\overline{x}^k\right)\ ,$$

$$P(\mathbf{x}_h, M) = \mathcal{T}\,\sqrt{(D_{11})^2 + (D_{22})^2 + (C_1)^2 + (C_2)^2}$$

$\Rightarrow$ MMPDEs are derived from variational principles as a minimiser of mapping functional

$$\mathcal{I}[\overline{\mathrm{x}}] = \frac{1}{2}\int_{\mathcal{D}_p} \sum_{k=1}^{2} (\nabla \overline{x}^k)^T\, M^{-1}\,\nabla \overline{x}^k\, d\mathbf{x}$$

$$\left(\text{In 1D:}\ \ \mathcal{I}[\overline{x}] = \frac{1}{2}\int_{\mathcal{D}_p} \frac{1}{q}\left(\frac{\partial \overline{x}}{\partial x}\right)^2 dx\ ,\ \text{ with the Euler-Lagrange equation: }\ \frac{\partial \overline{x}}{\partial x} = q\,\mathrm{C}\right)$$

Moving mesh apparatus

MMPDEs (see Huang, JCP 2001) govern time-dependent mapping of horizontal coordinates from transformed to physical space $\mathbf{x}_h = \mathbf{x}_h(\overline{\mathbf{x}}_h, \overline{t})$:

$$P(\mathbf{x}_h, M)\,\frac{\partial \mathbf{x}_h}{\partial \overline{t}} = \sum_{i,j=1,2} D_{ij}(\mathbf{x}_h, M)\,\frac{\partial^2 \mathbf{x}_h}{\partial \overline{x}^i \partial \overline{x}^j} + \sum_{i=1,2} C_i(\mathbf{x}_h, M)\,\frac{\partial \mathbf{x}_h}{\partial \overline{x}^i}$$

with coefficients

$$D_{ij}(\mathbf{x}_h, M) = \nabla_h\,\overline{x}^i \cdot M^{-1}\,\nabla_h\,\overline{x}^j \;, \qquad C_i(\mathbf{x}_h, M) = -\nabla_h\,\overline{x}^i \cdot \left(\sum_{k=1,2} \frac{\partial M^{-1}}{\partial \overline{x}^k} \nabla_h\,\overline{x}^k \right) \;,$$

$$P(\mathbf{x}_h, M) = \mathcal{T}\,\sqrt{(D_{11})^2 + (D_{22})^2 + (C_1)^2 + (C_2)^2}$$

$\Rightarrow$ MMPDEs are derived from variational principles as a minimiser of mapping functional

$$\mathcal{I}[\overline{\mathbf{x}}] = \frac{1}{2} \int_{\mathcal{D}_p} \sum_{k=1}^{2} (\nabla \overline{x}^k)^T\, M^{-1}\, \nabla \overline{x}^k \, d\mathbf{x}$$

$\left(\text{In 1D:} \;\; \mathcal{I}[\overline{x}] = \frac{1}{2} \int_{\mathcal{D}_p} \frac{1}{q} \left(\frac{\partial \overline{x}}{\partial x} \right)^2 dx \;, \text{ with the Euler-Lagrange equation: } \frac{\partial \overline{x}}{\partial x} = q\,\mathrm{C} \right)$

MMPDEs (see Huang, JCP 2001) govern time-dependent mapping of horizontal coordinates from transformed to physical space $\mathbf{x}_h = \mathbf{x}_h(\overline{\mathbf{x}}_h, \overline{t})$:

$$P(\mathbf{x}_h, M)\,\frac{\partial \mathbf{x}_h}{\partial \overline{t}} = \sum_{i,j=1,2} D_{ij}(\mathbf{x}_h, M)\,\frac{\partial^2 \mathbf{x}_h}{\partial \overline{x}^i \partial \overline{x}^j} + \sum_{i=1,2} C_i(\mathbf{x}_h, M)\,\frac{\partial \mathbf{x}_h}{\partial \overline{x}^i}$$

with coefficients

$$D_{ij}(\mathbf{x}_h, M) = \nabla_h \overline{x}^i \cdot M^{-1}\,\nabla_h \overline{x}^j \;, \qquad C_i(\mathbf{x}_h, M) = -\nabla_h \overline{x}^i \cdot \left(\sum_{k=1,2} \frac{\partial M^{-1}}{\partial \overline{x}^k} \nabla_h \overline{x}^k \right) \;,$$

$$P(\mathbf{x}_h, M) = \mathcal{T}\,\sqrt{(D_{11})^2 + (D_{22})^2 + (C_1)^2 + (C_2)^2}$$

$\Rightarrow$ MMPDEs are derived from variational principles as a minimiser of mapping functional

$$\mathcal{I}[\overline{\mathbf{x}}] = \frac{1}{2} \int_{\mathcal{D}_p} \sum_{k=1}^{2} (\nabla \overline{x}^k)^T\, M^{-1}\, \nabla \overline{x}^k \, d\mathbf{x}$$

$$\left(\text{In 1D:} \;\; \mathcal{I}[\overline{x}] = \frac{1}{2} \int_{\mathcal{D}_p} \frac{1}{q} \left(\frac{\partial \overline{x}}{\partial x} \right)^2 dx \;, \;\; \text{with the Euler-Lagrange equation:} \;\; \frac{\partial \overline{x}}{\partial x} = q\,\mathrm{C} \right)$$

Moving mesh apparatus

→ monitor function M (2×2 matrix in 2D):

$$M = I\, q$$

with scalar weighting function

$$q(t, \mathbf{x}_h) = 1 + \frac{\beta}{1-\beta}\,\frac{\Phi}{\langle\Phi\rangle_h}\,, \qquad I \text{ is identity matrix}$$

→ Φ is mesh refinement indicator; $\langle\Phi\rangle_h$ denotes its horizontal average

→ $0 \leq \beta < 1$ controls strength of adaptation

→ q is filtered to obtain good quality mesh

→ boundary conditions of 2D MMPDEs are either of Dirichlet-type for $\mathbf{x}_h$ found by means of one-dimensional MMPDEs

$$p(s,\mu)\,\frac{\partial s}{\partial t} = \mu\,\frac{\partial^2 s}{\partial \overline{s}^2} + \frac{\partial \mu}{\partial \overline{s}}\,\frac{\partial s}{\partial \overline{s}}$$

along boundary segments or are assumed periodic, depending on BCs in EULAG

Moving mesh apparatus

→ monitor function M (2×2 matrix in 2D):

$$M = I\, q$$

with scalar weighting function

$$q(t, \mathbf{x}_h) = 1 + \frac{\beta}{1-\beta}\, \frac{\Phi}{\langle \Phi \rangle_h}\ , \qquad I \text{ is identity matrix}$$

→ Φ is mesh refinement indicator; $\langle \Phi \rangle_h$ denotes its horizontal average

→ $0 \leq \beta < 1$ controls strength of adaptation

→ q is filtered to obtain good quality mesh

→ boundary conditions of 2D MMPDEs are either of Dirichlet-type for $\mathbf{x}_h$ found by means of one-dimensional MMPDEs

$$p(s,\mu)\, \frac{\partial s}{\partial \bar{t}} = \mu\, \frac{\partial^2 s}{\partial \bar{s}^2} + \frac{\partial \mu}{\partial \bar{s}}\, \frac{\partial s}{\partial \bar{s}}$$

along boundary segments or are assumed periodic, depending on BCs in EULAG

Flux-form NFT integration under moving meshes

Advective scalar transport equation in conservation form:

$$\frac{\partial(\rho^* \psi)}{\partial \bar{t}} + \overline{\nabla} \cdot (\rho^* \overline{\mathbf{v}}^* \psi) = 0$$

$\psi \equiv 1$ gives associated mass conservation law:

$$\frac{\partial \rho^*}{\partial \bar{t}} + \overline{\nabla} \cdot (\rho^* \overline{\mathbf{v}}^*) = 0$$

$\rightarrow$ We denote it as generalised anelastic mass conservation law (GMCL)

Equivalence with evolution equation

$$\frac{d\psi}{d\bar{t}} = 0 \qquad \text{where} \qquad d/d\bar{t} = \partial/\partial\bar{t} + \overline{\mathbf{v}}^* \cdot \overline{\nabla}$$

Without validity of GMCL:

$$\frac{d\psi}{d\bar{t}} = -\frac{\psi}{\rho^*}\left(\frac{\partial \rho^*}{\partial \bar{t}} + \overline{\nabla} \cdot (\rho^* \overline{\mathbf{v}}^*)\right)$$

Required properties of flux-form NFT MPDATA integration

- $\rightarrow$ Satisfy GMCL in integration
- $\rightarrow$ MPDATA compatibility with GMCL ($\Rightarrow$ preserve uniform field $\tilde{\psi} \equiv 1$)

Flux-form NFT integration under moving meshes

Advective scalar transport equation in conservation form:

$$\frac{\partial(\rho^* \psi)}{\partial \bar{t}} + \overline{\nabla} \cdot \left(\rho^* \overline{\mathbf{v}}^* \psi\right) = 0$$

$\psi \equiv 1$ gives associated mass conservation law:

$$\frac{\partial \rho^*}{\partial \bar{t}} + \overline{\nabla} \cdot \left(\rho^* \overline{\mathbf{v}}^*\right) = 0$$

$\rightarrow$ We denote it as generalised anelastic mass conservation law (GMCL)

Equivalence with evolution equation

$$\frac{d\psi}{d\bar{t}} = 0 \qquad \text{where} \qquad d/d\bar{t} = \partial/\partial\bar{t} + \overline{\mathbf{v}}^* \cdot \overline{\nabla}$$

Without validity of GMCL:

$$\frac{d\psi}{d\bar{t}} = -\frac{\psi}{\rho^*}\left(\frac{\partial \rho^*}{\partial \bar{t}} + \overline{\nabla} \cdot \left(\rho^* \overline{\mathbf{v}}^*\right)\right)$$

Required properties of flux-form NFT MPDATA integration

- $\rightarrow$ Satisfy GMCL in integration
- $\rightarrow$ MPDATA compatibility with GMCL ($\Rightarrow$ preserve uniform field $\tilde{\psi} \equiv 1$)

Flux-form NFT integration under moving meshes

GMCL can be decomposed using $\overline{\mathbf{v}}^* = \overline{\mathbf{v}}^s + \overline{\mathbf{v}}^g$ into generalised form of geometric conservation law (GCL) and anelastic mass continuity equation:

$$\frac{\partial \rho^*}{\partial \bar{t}} + \overline{\nabla} \cdot \left(\rho^* \overline{\mathbf{v}}^*\right) = \frac{\partial \rho^*}{\partial \bar{t}} + \overline{\nabla} \cdot \left(\rho^* \overline{\mathbf{v}}^g\right) + \overline{\nabla} \cdot \left(\rho^* \overline{\mathbf{v}}^s\right) = 0$$

Formulation of EULAG anelastic solver accounts for:

$$\overline{\nabla} \cdot \left(\rho^* \overline{\mathbf{v}}^s\right) = 0 \quad (< \ \epsilon)$$

However geometric conservation law

$$\frac{\partial \rho^*}{\partial \bar{t}} + \overline{\nabla} \cdot \left(\rho^* \overline{\mathbf{v}}^g\right) = 0$$

is not rigourously accounted for in the standard solver.

Combine NFT scheme MPDATA with solution-adaptive moving mesh

→ Three extensions have been developed to NFT MPDATA integration for its use with adaptive moving meshes (Kühnlein et al., JCP 2012):

1. $\mathcal{O}(\delta t^2)$ estimate of contravariant momentum flux $(\rho^* \overline{\mathbf{v}}^*)^{n+1/2}$ in MPDATA

   - compute as $(\rho^* \overline{\mathbf{v}}^*)^{n+1/2} = (\rho^* \overline{\mathbf{v}}^s)^{n+1/2} + (\rho^* \overline{\mathbf{v}}^g)^{n+1/2}$

   - use predictor for solenoidal part, e.g. linear: $(\rho^* \overline{\mathbf{v}}^s)^{n+1/2} = (1+\beta)\,(\rho^* \overline{\mathbf{v}}^s)^{n} - \beta\,(\rho^* \overline{\mathbf{v}}^s)^{n-1}$

   - mesh velocity $(\overline{\mathbf{v}}^g)^{n+1/2}$ and $\rho^{*\,n+1/2}$ obtained from $(\mathbf{v}^g)^{n+1/2} = (\mathbf{x}^{n+1} - \mathbf{x}^n)/\delta \overline{t}$, $\mathbf{x}^{n+1/2} = 0.5\,(\mathbf{x}^{n+1} + \mathbf{x}^n)$ and Kronecker delta relations for transformation

   - procedure minimises errors with respect to numerical representation of GCL in FT solver

2. density-correction factor in MPDATA pseudo-velocities

   - default MPDATA not exactly compatible with GMCL for general moving meshes

   - exact compatibility achieved for arbitrary moving meshes by introducing density-correction factor $\left(\rho_{\mathbf{i}}^{*n}/\rho_{\mathbf{i}}^{*n+1}\right)$ in error-compensative pseudo-velocities

   - pseudo-velocities retain form of original expressions but redefine entering field $\psi_{\mathbf{i}}^{(k-1)}$ as $\widehat{\psi}_{\mathbf{i}}^{(k-1)} := \psi_{\mathbf{i}}^{(k-1)}\left(\rho_{\mathbf{i}}^{*n}/\rho_{\mathbf{i}}^{*n+1}\right)$

   - maintains second-order asymptotic accuracy of MPDATA as with original pseudo-velocities

Combine NFT scheme MPDATA with solution-adaptive moving mesh

→ Three extensions have been developed to NFT MPDATA integration for its use with adaptive moving meshes (Kühnlein et al., JCP 2012):

1. $\mathcal{O}(\delta t^2)$ estimate of contravariant momentum flux $(\rho^* \overline{\mathbf{v}}^*)^{n+1/2}$ in MPDATA

   - compute as $(\rho^* \overline{\mathbf{v}}^*)^{n+1/2} = (\rho^* \overline{\mathbf{v}}^s)^{n+1/2} + (\rho^* \overline{\mathbf{v}}^g)^{n+1/2}$

   - use predictor for solenoidal part, e.g. linear: $(\rho^* \overline{\mathbf{v}}^s)^{n+1/2} = (1+\beta)\,(\rho^* \overline{\mathbf{v}}^s)^n - \beta\,(\rho^* \overline{\mathbf{v}}^s)^{n-1}$

   - mesh velocity $(\overline{\mathbf{v}}^g)^{n+1/2}$ and $\rho^{*\,n+1/2}$ obtained from $(\mathbf{v}^g)^{n+1/2} = (\mathbf{x}^{n+1} - \mathbf{x}^n)/\delta\bar{t}$, $\mathbf{x}^{n+1/2} = 0.5\,(\mathbf{x}^{n+1} + \mathbf{x}^n)$ and Kronecker delta relations for transformation

   - procedure minimises errors with respect to numerical representation of GCL in FT solver

2. density-correction factor in MPDATA pseudo-velocities

   - default MPDATA not exactly compatible with GMCL for general moving meshes

   - exact compatibility achieved for arbitrary moving meshes by introducing density-correction factor $\left(\rho_{\mathbf{i}}^{*n}/\rho_{\mathbf{i}}^{*n+1}\right)$ in error-compensative pseudo-velocities

   - pseudo-velocities retain form of original expressions but redefine entering field $\psi_{\mathbf{i}}^{(k-1)}$ as $\widehat{\psi}_{\mathbf{i}}^{(k-1)} := \psi_{\mathbf{i}}^{(k-1)}\left(\rho_{\mathbf{i}}^{*n}/\rho_{\mathbf{i}}^{*n+1}\right)$

   - maintains second-order asymptotic accuracy of MPDATA as with original pseudo-velocities

3. Elliptic solution approach for the generalised geometric conservation law (GCL)

- semi-discretised vectorial representation: $\frac{(\rho^{*n+1} - \rho^{*n})}{\delta \bar{t}} + \overline{\nabla} \cdot \left(\rho^* \overline{\mathbf{v}}^g\right)^{n+1/2} = 0$

- with prescribed ρ^{*n} and ρ^{*n+1}, a preliminary guess $\overline{\mathbf{v}}^g_*$ for the mesh velocity $\overline{\mathbf{v}}^g$ is corrected to satisfy this equation

- this is achieved by introducing a potential ϕ as

$$\left\{\overline{\mathbf{v}}^g = \overline{\mathbf{v}}^g_* - \widetilde{\mathbf{G}}^T \widetilde{\mathbf{G}}\, \overline{\nabla} \phi\right\}_{\mathbf{i}}^{n+1/2}$$

which leads to elliptic boundary value problem

$$\left\{-\frac{\delta \bar{t}}{\rho^{*n+1/2}} \left(\frac{(\rho^{*n+1} - \rho^{*n})}{\delta \bar{t}} + \overline{\nabla} \cdot \left(\rho^* \left[\overline{\mathbf{v}}^g_* - \widetilde{\mathbf{G}}^T \widetilde{\mathbf{G}}\, \overline{\nabla} \phi\right]\right)^{n+1/2}\right)\right\}_{\mathbf{i}} = 0$$

- solve with iterative GCR solver until residual $< \epsilon$

Time-dependent deformational shear flow (Blossey and Durran, JCP 2008):

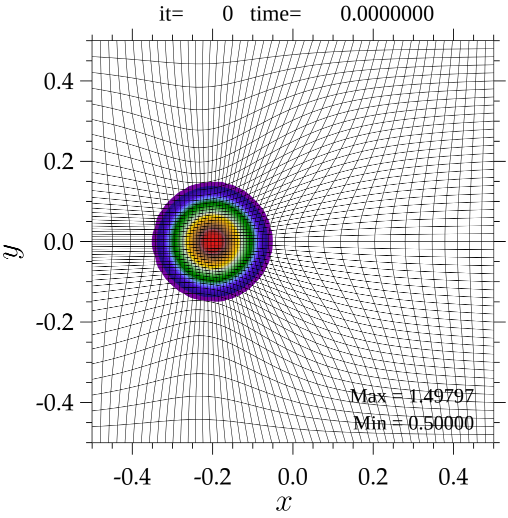

$\rightarrow$ mesh refinement indicator: $\Phi = ||\nabla_h \psi||$

Scalar advection numerical experiments

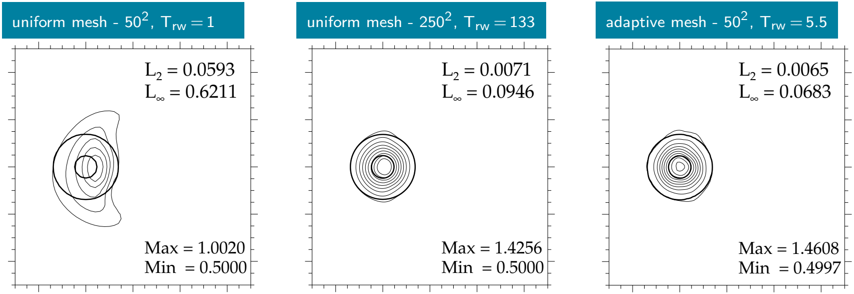

→ T_{rw} is relative wall clock computing time to uniform mesh run with 50^2 mesh cells (leftmost panel)

Scalar advection numerical experiments

scheme OS

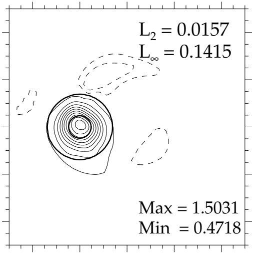

scheme RS

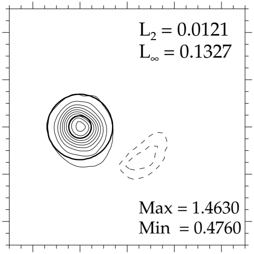

scheme RD

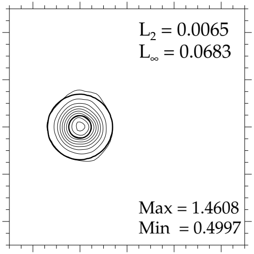

→ Solution-adaptive moving mesh simulations with different implementations of the NFT scheme MPDATA:

Implementation	Density-correction	GCL formulation
OS	No	standard
RS	Yes	standard
RD	Yes	diagnostic

Baroclinic wave life cycle experiments

- → zonally-periodic channel 10000 km × 8000 km × 18 km
- → baroclinically unstable jet flow in dry and inviscid atmosphere (Bush and Peltier, JAS 1994)
- → f-plane
- → perturb initial state by local θ-anomaly at tropopause
- → integrate for 12 days
- → mesh refinement indicator:

  $\Phi = 1/H \int_{z=0}^{H} \|\nabla_h \theta\| \, dz$

- → see Kühnlein et al., JCP 2012 for details

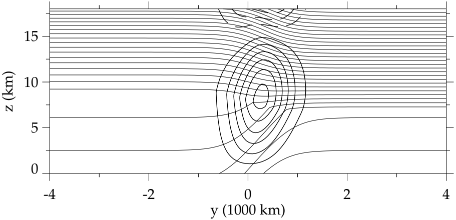

Baroclinic wave life cycle experiments

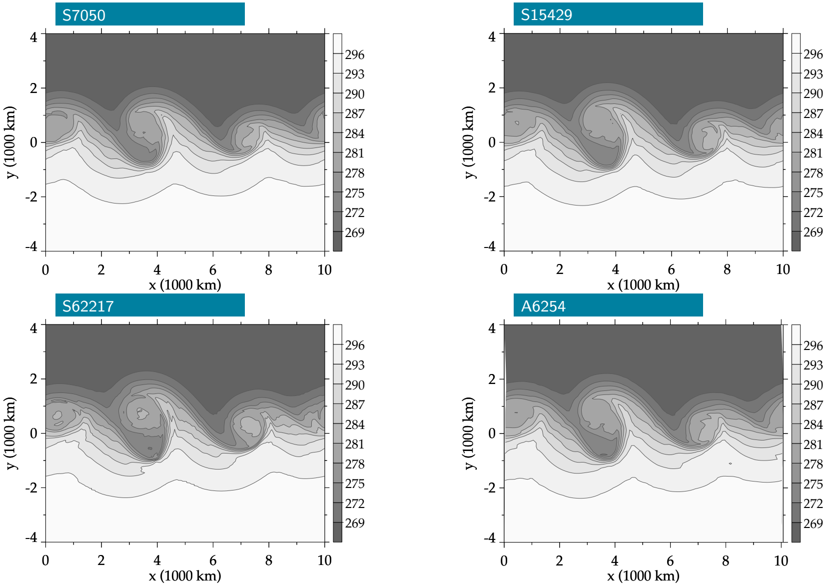

temperature field at $z = 2$ km and $t = 234$ h

Domain-averaged kinetic energetics with integration time

total kinetic energy $\langle \mathrm{KE} \rangle$

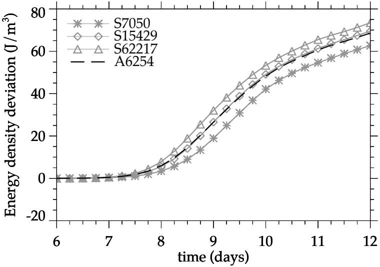

zonal kinetic energy $\langle \mathrm{ZKE} \rangle$

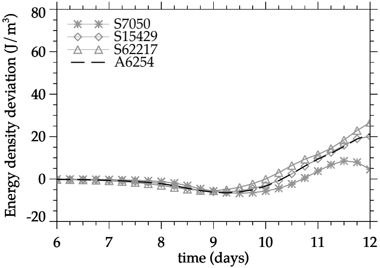

eddy kinetic energy $\langle \mathrm{EKE} \rangle$

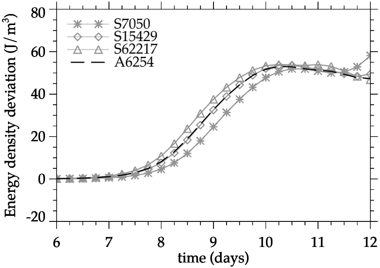

Sensitivity to mesh-refinement indicator

Simulation	Refinement indicator $\Phi(t,x,y)$	$\mathcal{E}_{\langle\mathrm{KE}\rangle}$	$\mathcal{E}_{\langle\mathrm{ZKE}\rangle}$	$\mathcal{E}_{\langle\mathrm{EKE}\rangle}$
S7050	-	6.43	4.99	4.84
S15429	-	2.58	1.66	1.90
A6254a	$\frac{1}{H}\int_0^H \lVert\nabla_h\theta\rVert\,dz$	2.82	1.67	1.80
A6254b	$\lVert\nabla_h\theta(z=600\text{ m})\rVert$	3.75	2.64	2.28
A6254c	$\lVert\nabla_h\theta(z=3000\text{ m})\rVert$	2.91	1.57	1.92
A6254d	$\lVert\nabla_h\theta(z=5100\text{ m})\rVert$	2.98	2.43	1.98
A6254e	$\frac{1}{H}\int_0^H \lVert\nabla\times\mathbf{v}\rVert\,dz$	2.90	2.10	1.83
A6254f	$\frac{1}{H}\int_0^H \lvert PV\rvert\,dz$	3.81	2.31	2.45
A6254g	$\lvert PV(z=5100\text{ m})\rvert$	4.65	2.48	2.97
A6254h	$\lvert PV(z=9000\text{ m})\rvert$	4.22	2.62	2.64
A6254i	$\frac{1}{H}\int_0^H \lVert\nabla_h PV\rVert\,dz$	3.82	2.36	2.65
A6254j	$\frac{1}{H}\int_0^H \lvert PV\rvert\,dz,\ \frac{1}{H}\int_0^H \lVert\nabla_h PV\rVert\,dz$	3.84	2.27	2.52
A6254k	$\frac{1}{H}\int_0^H \lvert EPV\rvert\,dz$	10.77	5.43	8.57
A6254l	$\lvert EPV(z=5100\text{ m})\rvert$	9.50	4.60	7.56

$$\mathcal{E}_\vartheta = \left(\frac{1}{N_o}\sum_{i=1}^{N_o}\left(\vartheta_i - \vartheta_i^R\right)^2\right)^{1/2} \qquad \forall\quad \vartheta = \langle\mathrm{KE}\rangle\,,\langle\mathrm{ZKE}\rangle\,,\langle\mathrm{EKE}\rangle$$

$\rightarrow$ ϑ^R is high-resolution reference simulation S62217 with static uniform mesh
$\rightarrow$ $N_o = 48$ is number of 6-hourly model outputs over integration period of 12 days

Multiscale performance

→ Representation of internal gravity waves occurring in response to imbalances in the evolving baroclinic wave flow:

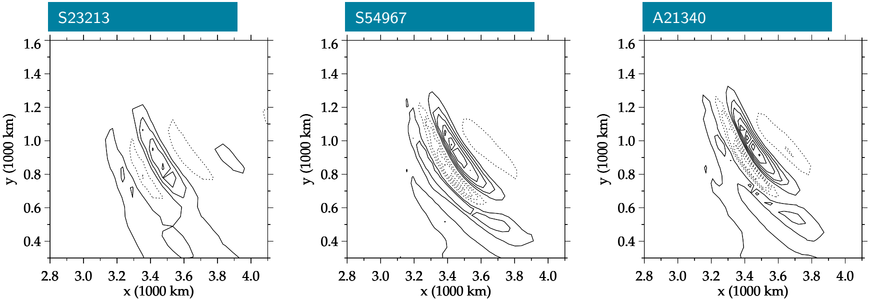

vertical velocity field at $z = 12$ km and $t = 246$ h

Outlook

→ application to 3D atmospheric flows including moist processes (moist baroclinic wave life cycle, single moist bubble, mesoscale convective storm)

→ extension of solution-adaptive moving meshes to the sphere for simulating global atmospheric flows

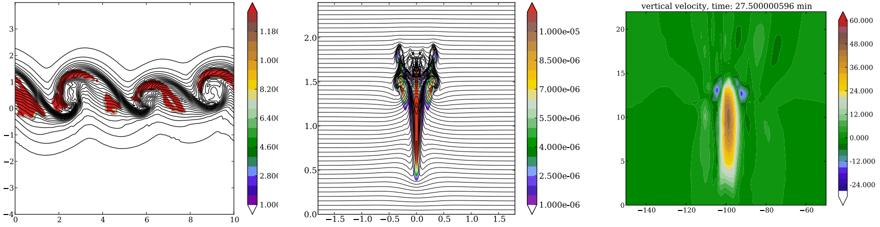

⇒ Special thanks to: George Craig, Joseph Prusa, Ulrich Schumann, and Andii Wyszogrodzki

Outlook

→ application to 3D atmospheric flows including moist processes (moist baroclinic wave life cycle, single moist bubble, mesoscale convective storm)

→ extension of solution-adaptive moving meshes to the sphere for simulating global atmospheric flows

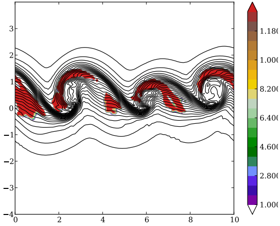

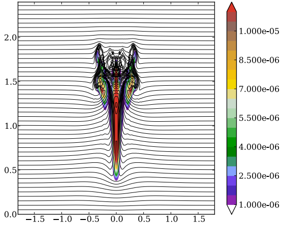

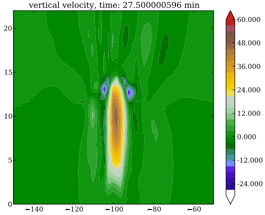

⇒ Special thanks to: George Craig, Joseph Prusa, Ulrich Schumann, and Andii Wyszogrodzki